# Understanding the nonlinear phase and frequency shift of an ultrashort light pulse induced by an inertial third-order optical nonlinearity

A. M. Zheltikov
*Physics Department, International Laser Center, M. V. Lomonosov Moscow State University, Vorob'evy gory, Moscow 119992, Russia*
(Received 27 September 2008; published 19 February 2009)

Inertia of optical nonlinearity is shown to distort the temporal profile of the intensity-dependent phase shift of an ultrashort laser pulse relative to the phase induced by the instantaneous optical nonlinearity. We demonstrate that a weakly inertial optical nonlinearity, whose response time is smaller than the pulse width, tends to redshift the light field and generates a cubic-phase correction to the quadratic phase, thus complicating the chirp of the spectrally broadened field. For very short light pulses with pulse widths shorter than the response times of optical nonlinearity, the redshift and cubic-phase terms often dominate the nonlinear phase shift, giving rise to phase profiles significantly different from those induced by instantaneous optical nonlinearity.

DOI: 10.1103/PhysRevA.79.023823 PACS number(s): 42.65.Dr, 42.65.Re

## I. INTRODUCTION

Methods of ultrafast nonlinear optics are at the heart of rapidly advancing laser technologies, helping to provide an unprecedented precision in controlled synthesis of ultrashort field waveforms [1]. Nonlinear-optical techniques enable transformation of ultrashort pulses into octave-spanning supercontinua [2,3] and offer ways of compressing light fields to single-cycle and subcycle pulse widths [4], giving a powerful momentum to the development of ultrafast spectroscopy [5,6], optical metrology [7], microscopy [8], and bioimaging [9], as well as stimulating experimental and theoretical studies of basic physical phenomena behind diversified regimes of spectral and temporal transformations of ultrashort light pulses in highly nonlinear dispersive systems [10–17].

A standard nonlinear-optical technique of pulse compression is based on self-phase-modulation due to the fast electron, Kerr-type optical nonlinearity [18]. Nonlinearity of this type induces an ultrafast-response change in the refractive index of a medium, which almost instantaneously follows the temporal envelope of the pulse intensity. In this regime, the spectral broadening of a light pulse with a symmetric temporal envelope is symmetric with respect to its central frequency. The related chirp of the laser field is then dominated by a linear term about the peak of the laser pulse, enabling efficient pulse compression through linear chirp compensation by an anomalously dispersive medium or structure. This method of pulse compression has been successfully used in ultrafast laser technologies over the past two decades, allowing the generation of light pulses as short as a few field cycles [19].

In the case of intense few-cycle light pulses, however, spectral broadening scenarios tend to become more complicated [20–22], involving shock-wave formation and ionization-induced broadening in addition to the Kerr effect, and often showing an increasing sensitivity to high-order dispersion effects. Remarkably, these more involved scenarios of nonlinear-optical pulse transformation offer unique possibilities for carrier-envelope-phase-controlled compression of high-intensity laser pulses down to few-cycle pulse widths [23,24]. While the shock-wave field dynamics and ionization-related phase shifts typically intensify the high-frequency wing of the spectrum, giving rise to a noticeable blueshifting of ultrashort light pulses [20–22,25–27], the long-wavelength part of the spectrum can be enhanced by plasma-defocusing-induced pulse reshaping [28,29] and the retarded part of optical nonlinearity, related to the nonlinear-optical response of heavier particles and quasiparticles, such as molecules in the gas and liquid phase or phonons in solids [30,31]. Redshifting of light pulses due to the inertia of optical nonlinearity has been intensely studied over the past two decades for the anomalously dispersive regime of field evolution, where this effect is manifested as the soliton self-frequency-shift [32–34], offering attractive solutions for the creation of wavelength-tunable soliton fiber light sources. However, as elegantly explained by Santhanama and Agrawal [35], redshifting due to retarded optical nonlinearity is also effective in the regime of normal dispersion, suggesting ways to intensify the long-wavelength wing of spectrally transformed optical fields.

In this paper, we show that such an intensification of the low-frequency part of the spectrum in a medium with an inertial optical nonlinearity comes at the penalty of phase profile distortion. We will demonstrate that, in such a medium, the temporal profile of the intensity-dependent phase shift of an ultrashort laser pulse is distorted with respect to the phase profile induced by instantaneous optical nonlinearity. It will be shown that a weakly inertial optical nonlinearity, whose response time is smaller than the pulse width, tends to redshift the light field and generates a cubic-phase correction to the quadratic phase, thus complicating the chirp of the spectrally broadened field. For very short light pulses with pulse widths shorter than the response times of optical nonlinearity, the redshift and cubic-phase terms often dominate the nonlinear phase shift, giving rise to phase profiles significantly different from those induced by instantaneous optical nonlinearity.

## II. PHASE SHIFT BY INSTANTANEOUS AND INERTIAL OPTICAL NONLINEARITIES

We start our analysis with the generic expression for the phase shift induced by the third-order optical nonlinearity [30,31,36]

 

$$\varphi(\eta,z) = -k_0 n_2 z \int_{-\infty}^{\eta} I(\xi) R(\eta-\xi) d\xi, \tag{1}$$

where $k_0=2\pi/\lambda$, $\lambda$ is the radiation wavelength, $n_2$ is the nonlinear refractive index of the medium, $z$ is the propagation coordinate, $\eta$ is the retarded time, $I(\eta)$ is the temporal profile of the field intensity, and $R(\theta)$ is the nonlinear-optical response of the medium [31,36],

$$R(\theta) = (1-f_R)\delta(\theta) + f_R H(\theta), \tag{2}$$

which includes the instantaneous Kerr-type nonlinearity, represented by the $\delta$-function term, and the inertial nonlinear response $H(\theta)$ which enters into Eq. (2) with its weighing factor $f_R$, quantifying the fraction of retarded nonlinearity in the overall nonlinear-optical response.

Substituting Eq. (2) into Eq. (1), we express the overall nonlinear phase shift as a sum of the instantaneous Kerr-type response and the phase induced by the retarded part of optical nonlinearity:

$$\varphi(\eta,z) = \varphi_K(\eta,z) + \varphi_R(\eta,z), \tag{3}$$

where

$$\varphi_K(\eta,z) = -k_0 n_2 z (1-f_R) I(\eta), \tag{4}$$

$$\varphi_R(\eta,z) = -k_0 n_2 z f_R \int_{-\infty}^{\eta} I(\xi) H(\eta-\xi) d\xi. \tag{5}$$

Equation (4) gives a standard expression for the nonlinear phase shift related to the instantaneous Kerr-type optical nonlinearity, which scales linearly with $n_2$, $z$, and the peak intensity $I_0$, where $I(\eta)=I_0\psi(\eta)$ [$\psi(\eta)$ is the normalized temporal intensity profile]. In the region around the peak of a light pulse with an arbitrary temporal envelope, where the Taylor series expansion

$$\psi(\eta) \approx 1 + \frac{1}{2}\left.\frac{\partial^2\psi}{\partial\eta^2}\right|_{\eta=0}\eta^2 \tag{6}$$

holds true, the Kerr effect induces a purely linear chirp, with the deviation $\delta\omega(t)=\omega(t)-\omega_0$ of the instantaneous frequency $\omega(t)$ from the central frequency $\omega_0$ defined by

$$\delta\omega_K(t) = \partial\varphi_K/\partial t = -k_0 n_2 z I_0 (1-f_R)\partial\psi(\eta)/\partial\eta \approx k_0 n_2 z I_0 (1-f_R)\left.\frac{\partial^2\psi}{\partial\eta^2}\right|_{\eta=0}\eta. \tag{7}$$

In the particular case of a Gaussian pulse,

$$\psi(\eta) = \exp\left(-\frac{\eta^2}{\tau_p^2}\right), \tag{8}$$

the Kerr-effect-induced phase shift (4) takes the form

$$\varphi_K(\eta,z) = -k_0 n_2 z (1-f_R) I_0 \exp\left(-\frac{\eta^2}{\tau_p^2}\right), \tag{9}$$

generating the linear chirp

$$\delta\omega_K(t) \approx 2k_0 n_2 z I_0 (1-f_R)\frac{\eta}{\tau_p^2} \tag{10}$$

around the peak of the light pulse, $\eta/\tau_p \ll 1$, where $\psi(\eta) \approx 1-\eta^2/\tau_p^2$.

Evaluation of the phase shift induced by the inertial nonlinearity requires knowledge of the response function $H(\theta)$. Here, we consider two generic models of the inertial nonlinear response $H(\xi)$. The first model assumes a monoexponential relaxation of optical nonlinearity with a relaxation time $\tau_{\rm nl}$,

$$H_1(\theta) = \frac{1}{\tau_{\rm nl}}\exp\left(-\frac{\theta}{\tau_{\rm nl}}\right)\Theta(\theta), \tag{11}$$

where $\Theta(t)$ is the Heaviside step function, and is often used to describe the inertial nonlinear-optical response of molecules in a liquid phase [30]. The second model describes the retarded part of optical nonlinearity as a damped oscillator,

$$H_2(\theta) = \frac{\tau_1^2+\tau_2^2}{\tau_1\tau_2^2}\sin\left(\frac{\theta}{\tau_1}\right)\exp\left(-\frac{\theta}{\tau_2}\right)\Theta(\theta), \tag{12}$$

and is broadly used to model the Raman response of optical fibers [31,34,36] and atmospheric air [20,21,37,38] In the case of a Gaussian pulse (8), calculation of the integral in Eq. (5) for the first and second models of the inertial nonlinear-optical response gives

$$\varphi_{R1}(\eta,z) = -k_0 n_2 z f_R I_0 \frac{\sqrt{\pi}}{2}\frac{\tau_p}{\tau_{\rm nl}} \times \exp\left(\frac{\tau_p^2}{4\tau_{\rm nl}^2}\right)\exp\left(-\frac{\eta}{\tau_{\rm nl}}\right)\mathrm{erfc}\left(\frac{\tau_p}{2\tau_{\rm nl}}-\frac{\eta}{\tau_p}\right), \tag{13}$$

$$\varphi_{R2}(\eta,z) = -k_0 n_2 z f_R i I_0 \frac{\sqrt{\pi}}{4}\frac{\tau_p(\tau_1^2+\tau_2^2)}{\tau_1\tau_2^2} \times\left\{\exp\left[\frac{\tau_p^2}{4}\left(\frac{1}{\tau_2}-\frac{2\eta}{\tau_p^2}+\frac{i}{\tau_1}\right)^2\right] \times\mathrm{erfc}\left[\frac{\tau_p}{2}\left(\frac{1}{\tau_2}-\frac{2\eta}{\tau_p^2}+\frac{i}{\tau_1}\right)\right] -\exp\left[\frac{\tau_p^2}{4}\left(\frac{1}{\tau_2}-\frac{2\eta}{\tau_p^2}-\frac{i}{\tau_1}\right)^2\right] \times\mathrm{erfc}\left[\frac{\tau_p}{2}\left(\frac{1}{\tau_2}-\frac{2\eta}{\tau_p^2}-\frac{i}{\tau_1}\right)\right]\right\}, \tag{14}$$

where $\mathrm{erfc}(\theta)=1-2(\pi)^{-1/2}\int_0^{\theta}\exp(-\xi^2)d\xi$ is the complementary error function.

In the following sections, we will consider in greater detail two limiting regimes corresponding to weakly and strongly inertial optical nonlinearities. In the former regime, the pulse width $\tau_p$ is much larger than the response times of optical nonlinearity, while in the latter case, the opposite inequalities, $\tau_p \ll \tau_{\rm nl}, \tau_1, \tau_2$ hold true. It is instructive to apply these relations between the pulse width and the times characterizing the inertia of optical nonlinearity to define the lim-

its of weak and strong inertia of optical nonlinearity for materials widely used in optical science and technology. The damped-oscillator model of Eq. (12) provides a reasonable approximation for the description of the rotational Raman response of the atmospheric air, as well as the inertial nonlinearity related to optical phonons in fused silica, silicon, diamond and many other materials. For the rotational Raman response of the atmospheric air, for example, $\tau_1 \approx 62.5$ fs and $\tau_2 \approx 77$ fs, implying that, for light pulses with $\tau_p \leqslant 10$ fs, this type of optical nonlinearity qualifies as strongly inertial, while for pulses with $\tau_p \geqslant 300$ fs, this nonlinearity can be considered as weakly inertial. In the case of a Raman response of fused silica, $\tau_1 \approx 12.5$ fs and $\tau_2 \approx 32$ fs, such a nonlinearity can be treated as weakly inertial for $\tau_p \geqslant 100$ fs and strongly inertial for sub-5-fs pulses. For the longitudinal optical phonon of silicon, $\tau_1 \approx 10$ fs and $\tau_2 \approx 3$ ps, the inertia of the nonlinear-optical response is weak for pulses longer than 50–60 fs. Finally, for the 1331 $cm^{-1}$ optical phonon of diamond, $\tau_1 \approx 4$ fs and $\tau_2 \approx 6.7$ ps, and the nonlinear-optical response is weakly inertial even for pulses as short as 20–30 fs. Equation (11), on the other hand, is often used to describe the Raman response of molecules in the liquid phase. The orientation relaxation time for such molecules typically lies in the picosecond range (e.g., a good fit for the spectra of picosecond laser pulses broadened in $CS_2$ is achieved with $\tau_{nl} \approx 9$ ps [30]). The inertia of such a nonlinearity qualifies as strong everywhere in the femtosecond range of pulse widths and can only be regarded as weak when pulses become longer than tens of picoseconds.

### III. WEAKLY INERTIAL OPTICAL NONLINEARITY

For a weakly inertial response, with $\tau_{nl}, \tau_1, \tau_2 \ll \tau_p$, an asymptotical expression $\mathrm{erfc}\,\zeta \approx \zeta^{-1}\pi^{-1/2}\exp(-\zeta^2)$, which is valid for large $\zeta$, reduces Eqs. (13) and (14) to

$$\varphi_{R1,2}(\eta,z) \approx -k_0 n_2 z f_R I_0 \exp\left(-\frac{\eta^2}{\tau_p^2}\right)\left(1+2\mu_{1,2}\frac{\eta}{\tau_p}\right), \tag{15}$$

where $\mu_1 = \tau_{nl}/\tau_p$ and $\mu_2 = \tau_p^{-1}\tau_2^{-1}(\tau_1^{-2}+\tau_2^{-2})^{-1}$ are small parameters. It is straightforward to verify that, in the case when $\tau_1 \gg \tau_2$, i.e., when an exponential decay dominates the response function $H_2(\theta)$, Eq. (15) gives identical results for $\varphi_{R1}(\eta,z)$ and $\varphi_{R2}(\eta,z)$ with $\tau_{nl} = \tau_2$. In Fig. 1, we compare the nonlinear phase shift $\varphi_{R1}(\eta,z)$ calculated with the use of Eq. (13) (open circles) and Eq. (15) (dashed line) for $\tau_{nl}/\tau_p = 0.1$. This comparison shows that Eq. (15) provides an excellent approximation for the phase shifts $\varphi_{R1,2}(\eta,z)$ induced by a weakly inertial optical nonlinearity near the peak of a light pulse.

As can be seen from comparison of Eqs. (9) and (15), in a linear approximation in a small parameter $\mu_1 = \tau_{nl}/\tau_p$ or $\mu_2 = \tau_p^{-1}\tau_2^{-1}(\tau_1^{-2}+\tau_2^{-2})^{-1}$, a weak inertia of the nonlinear-optical response is included in the nonlinear phase shift through a factor $1+2\mu_{1,2}\eta/\tau_p$. Around the peak of the pulse, $\eta/\tau_p \ll 1$, where $\psi(\eta) \approx 1-\eta^2/\tau_p^2$, this factor gives rise to linear ($\propto \mu_{1,2}\eta/\tau_p$) and cubic ($\propto \mu_{1,2}\eta^3/\tau_p^3$) phase terms in addition to the quadratic phase $\propto \eta^2/\tau_p^2$, which also appears in the

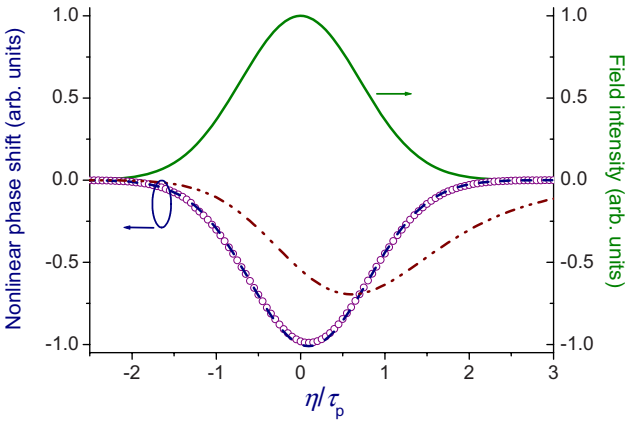


FIG. 1. (Color online) Temporal profile of the nonlinear phase shift $\varphi_{R1}$ induced by an inertial optical nonlinearity with $\tau_{nl}/\tau_p = 0.1$ (open circles and dashed line) and $\tau_{nl}/\tau_p = 1$ (dash-dotted line) calculated using Eq. (13) (open circles and dash-dotted line), and approximated by Eq. (15) (dashed line). Field intensity envelope is shown by the solid line.

expression for the Kerr-effect-related nonlinear phase $\varphi_K(\eta,z)$. The related frequency deviation around the peak of the pulse is

$$\delta\omega_{R1,2}(t) \approx 2k_0 n_2 z I_0 f_R\left[\frac{\eta}{\tau_p^2} - \frac{\mu_{1,2}}{\tau_p}\left(1-3\frac{\eta^2}{\tau_p^2}\right)\right]. \tag{16}$$

In addition to the linear chirp, represented by the $\propto \eta/\tau_p^2$ term in Eq. (16), the expression for $\delta\omega_{R1,2}(t)$ also includes small corrections implying a uniform frequency downshift $\propto -\mu_{1,2}/\tau_p$ and a quadratic chirp $\propto(\mu_{1,2}/\tau_p)(\eta/\tau_p)^2$. Continuous redshifting of ultrashort pulses induced by retarded optical nonlinearity has been earlier extensively studied for the regime of anomalous dispersion, where this effect is usually referred to as the soliton self-frequency-shift. In the solitonic regime, where the peak power of a soliton needs to scale as $\tau_s^{-2}$ with the soliton pulse width $\tau_s$ to keep the balance between dispersion and nonlinearity, the soliton frequency shift rate $\partial|\Delta f|/\partial z$ ($\Delta f$ is the soliton frequency shift) has been shown to scale as $\tau_s^{-4}$ as long as the Raman gain profile can be approximated with a linear function of radiation frequency. For nonsolitonic pulses, no balance between dispersion and nonlinearity is assumed, with the peak power scaling simply as $\tau_p^{-1}$ with the pulse width $\tau_p$, leading to a $\tau_p^{-3}$ scaling law for the rate of frequency downshift. This $\tau_p^{-3}$ scaling law has been elegantly explained by Santhanam and Agrawal [35] for the regime of normal dispersion by using the method of moment analysis. Both the $\tau_s^{-4}$ and $\tau_p^{-3}$ scaling laws for the rate of the frequency downshift of a light pulse are readily recovered by taking the derivative $\partial(|\delta\omega_{R1,2}|)/\partial z$ of the frequency shift defined by Eq. (16) with a substitution $I_0 = P/S \propto \tau_s^{-2}$ for the solitonic regime and $I_0 = P/S \propto \tau_p^{-1}$ for a nonsolitonic regime ($S$ being the effective beam area).

For light pulses with $\tau_p = 100$ fs, $I_0 \approx 10^{12}$ W/cm$^2$, and a central frequency $\omega_0$ propagating in fused silica ($\tau_1 \approx 12.5$ fs, $\tau_2 \approx 32$ fs, $n_2 \approx 3\times 10^{-16}$ cm$^2$/W, $f_R \approx 0.18$), Eq. (16) yields the following estimate for the redshift: $|\delta\omega_{R2}/\omega_0| \approx 10^{-3} z$ (cm) (where $z$ is expressed in centime-

ters). A light pulse with a central wavelength $\lambda_0=1$ $\mu$m will thus be redshifted by 100 nm within a propagation length of $z\approx 1$ m. Such propagation lengths are typical of many fiber experiments, where the redshifting of ultrashort light pulses is often quite substantial, especially in the soliton regime [39–42], in agreement with the above estimates.

In the case of fused silica or atmospheric air, the inertial nonlinearity constitutes only a certain fraction of the overall nonlinear-optical response (about 18% in the case of fused silica and about 50% for the atmospheric air). The redshifting of ultrashort pulses is therefore observed in such media simultaneously with spectral broadening due to the fast electronic nonlinearity (the Kerr effect). On the other hand, many liquids are known to feature strong Raman optical nonlinearities, which are almost entirely due to a strongly inertial molecular response, characterized by relatively long orientation relaxation times on the picosecond time scale. Pico- and subpicosecond pulses propagating in such media, as shown nearly four decades ago [30,43], tend to form small-scale filaments and undergo a well-pronounced redshifting (by 6–8 nm for 5 ps laser pulses transmitted through a cell filled with $CS_2$ [30,43]), with only a small fraction of energy contained in the blue wing of the spectrum.

## IV. EXTREMELY SHORT PULSES AND STRONGLY INERTIAL OPTICAL NONLINEARITY

In the opposite limiting case of extremely short light pulses and strongly inertial optical nonlinearity, $\tau_p \ll \tau_{\rm nl}, \tau_1, \tau_2$, integration in Eq. (5) with the response functions $H_{1,2}(\theta)$ defined by Eqs. (11) and (12) yields

$$\varphi_{R1,2}(\eta,z) \approx -k_0 n_2 z f_R I_0 \frac{\sqrt{\pi}}{2}\varepsilon_{1,2}\,\mathrm{erfc}\left(-\frac{\eta}{\tau_p}\right), \qquad (17)$$

where $\varepsilon_1=\mu_1^{-1}=\tau_p/\tau_{\rm nl}$ and $\varepsilon_2=\tau_1\mu_1^{-1}\tau_2^{-1}=\tau_p\tau_1(\tau_1^{-2}+\tau_2^{-2})$ are small parameters. Around the peak of the pulse, $\eta/\tau_p \ll 1$, a Taylor-series expansion erfc $\zeta \approx 1-2(\pi)^{-1/2}(\zeta-\zeta^3/3+\zeta^5/10)$ reduces Eq. (17) to

$$\varphi_{R1,2}(\eta,z) \approx -k_0 n_2 z f_R \varepsilon_{1,2} I_0 \left[\frac{\sqrt{\pi}}{2}+\frac{\eta}{\tau_p}-\frac{1}{3}\left(\frac{\eta}{\tau_p}\right)^3 + \frac{1}{10}\left(\frac{\eta}{\tau_p}\right)^5\right]. \qquad (18)$$

Figure 2 compares the nonlinear phase shift $\varphi_{R1}(\eta,z)$ calculated with the use of Eq. (13) (open circles) and Eq. (18) (dashed line) with $\tau_{\rm nl}/\tau_p=10$. As can be seen from this comparison, Eq. (18) provides an excellent approximation for the phase shifts $\varphi_{R1,2}(\eta,z)$ induced by a strongly inertial optical nonlinearity near the peak of a light pulse.

In contrast to the case of a weakly inertial nonlinear-optical response, the phase shifts $\varphi_{R1,2}(\eta,z)$ induced by a strongly inertial nonlinearity are intrinsically small because a short light pulse cannot efficiently drive an inertial optical nonlinearity with a response time much longer than the pulse width. Indeed, in the regime of a weakly inertial nonlinearity, the ratio of $|\varphi_{R1,2}(\eta,z)|$ to the Kerr-effect-related phase shift $|\varphi_K(\eta,z)|$ around the peak of the pulse, $\eta/\tau_p \ll 1$, is estimated, in accordance with Eqs. (4) and (15), simply as the ratio $f_R/(1-f_R)$, yielding a value of $\approx 1$ in the case of the rotational Raman response of the atmospheric air and $\approx 0.22$ for the Raman response of fused silica. For extremely short light pulses and strongly inertial optical nonlinearity, on the other hand, we find from Eqs. (4) and (18) that the ratio

$$|\varphi_{R1,2}(0,z)|/|\varphi_K(0,z)| \approx \frac{\sqrt{\pi}}{2}\frac{f_R}{1-f_R}\varepsilon_{1,2} \qquad (19)$$

is proportional to a small parameter $\varepsilon_{1,2}$. The $\varepsilon_{1,2}$ smallness of the phase shift $|\varphi_{R1,2}(\eta,z)|$ in the regime of extremely short light pulses and strongly inertial optical nonlinearity is illustrated in Fig. 2, where the nonlinear phase shift $|\varphi_{R1,2}(\eta,z)|$ is seen to decrease with the growth of the ratio $\tau_{\rm nl}/\tau_p$.

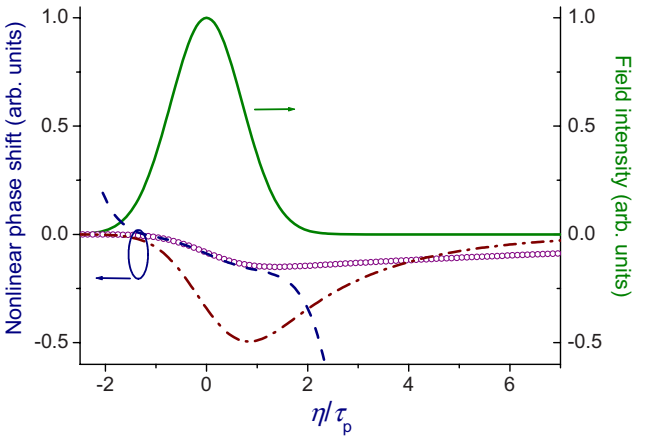


FIG. 2. (Color online) Temporal profile of the nonlinear phase shift $\varphi_{R1}$ induced by an inertial optical nonlinearity with $\tau_{\rm nl}/\tau_p=10$ (open circles and dashed line) and $\tau_{\rm nl}/\tau_p=2$ (dash-dotted line) calculated using Eq. (13) (open circles and dash-dotted line), and approximated by Eq. (18) (dashed line). Field intensity envelope is shown by the solid line.

It is straightforward to see from the comparison of Eqs. (15) and (18), as well as from Figs. 1 and 2, that the temporal profile of the nonlinear phase shift in the case of strongly inertial optical nonlinearity radically differs from both $\varphi_{R1,2}(\eta,z)$ in the regime of a weakly inertial optical nonlinearity and the temporal profile of the Kerr-effect-induced phase shift $\varphi_K(\eta,z)$. Since in the case of a strongly inertial nonlinear-optical response, the induced phase shift very substantially lags behind the light pulse, $\varphi_{R1,2}(\eta,z)$ is no longer dominated by a quadratic term, which plays a dominant role in the case of instantaneous optical nonlinearity (see, e.g., Refs. [18,19]).

The relevant frequency deviation is given by

$$\delta\omega_{R1,2}(\eta,z) \approx -k_0 n_2 z f_R \varepsilon_{1,2} I_0 \left[\frac{1}{\tau_p}-\left(\frac{\eta}{\tau_p}\right)^2+\frac{1}{2}\left(\frac{\eta}{\tau_p}\right)^4\right]. \qquad (20)$$

The first term in the square brackets in Eq. (20) describes a uniform frequency downshift of the laser field. The dependence of this frequency shift on the pulse width is less dramatic than in the regime of a weakly inertial nonlinearity

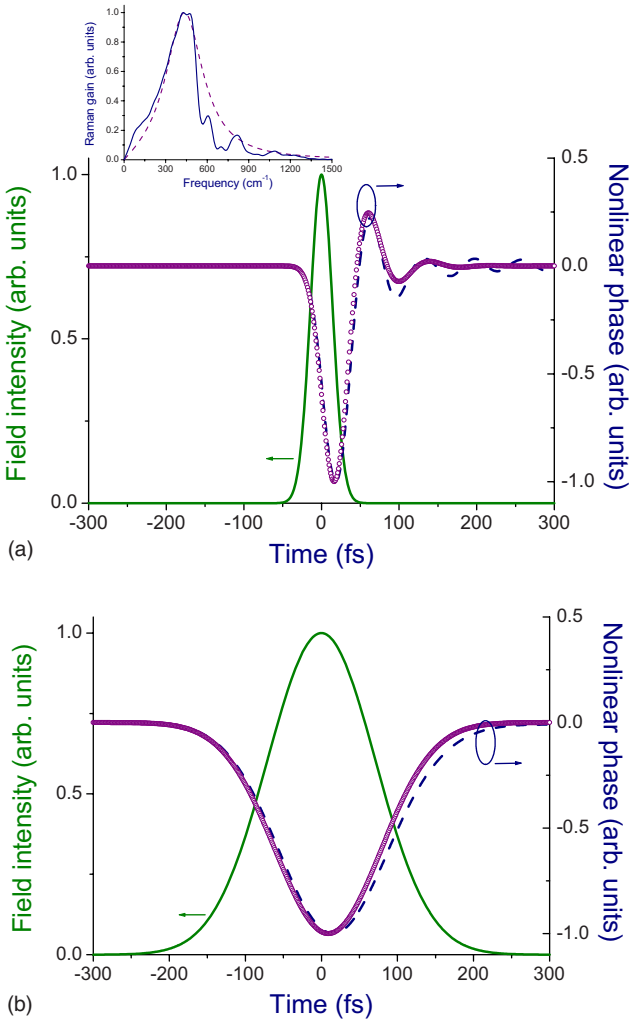


FIG. 3. (Color online) Temporal profile of the nonlinear phase shift $\varphi_R$ induced by an inertial optical nonlinearity with (circles) a single-oscillator response function [Eq. (12)] with $\tau_1=12.5$ fs and $\tau_2=32$ fs and (dashed line) the HC-model multiple-vibration-mode response as defined by Eq. (22). Field intensity envelope is shown by the solid line. The pulse width is 20 (a) and 100 (b) fs. The inset displays the Raman gain spectra for the single-damped-oscillator model [Eq. (12)] with $\tau_1=12.5$ fs and $\tau_2=32$ fs (dashed line) and the HC model (solid line).

as the pulse is already short enough for its bandwidth to cover the entire band of the nonlinear response, $\tau_p^{-1} \gg \tau_{\mathrm{nl}}^{-1}$. Importantly, while the nonlinear phase shift induced by a strongly inertial optical nonlinearity is $\varepsilon$ small, the related frequency shift is not. To examine the implications of this result, we consider a material with a response time of optical nonlinearity $\tau_{\mathrm{nl}}$. For light pulses with pulse widths $\tau_{p1} \gg \tau_{\mathrm{nl}}$, such an optical nonlinearity qualifies as weakly inertial, inducing a redshift with a $\mu$-small rate $\partial(|\delta\omega_{R1}|)/\partial z \approx 2k_0 n_2 I_0 f_R \mu_1/\tau_{p1} \ll k_0 n_2 I_0 f_R/\tau_{p1}$. For very short light pulses with pulse widths $\tau_{p2} \ll \tau_{\mathrm{nl}}$, on the other hand, optical nonlinearity becomes strongly inertial, and we apply Eq. (20) to find $\partial(|\delta\omega_{R1}|)/\partial z \approx k_0 n_2 I_0 f_R/\tau_{\mathrm{nl}}$, which is a factor of $\tau_{p1}/\tau_{\mathrm{nl}} \gg 1$ higher than the frequency shift rate in the regime of a weakly inertial nonlinearity.

In the case of ultrashort light pulses with $I_0 \approx 10^{14}$ W/cm$^2$ and a central frequency $\omega_0$ propagating in the atmospheric air ($\tau_1 \approx 62.5$ fs, $\tau_2 \approx 77$ fs, $n_2 \approx 5 \times 10^{-19}$ cm$^2$/W, $f_R \approx 0.5$), the redshift predicted by Eq. (20) is $|\delta\omega_{R2}/\omega_0| \approx 2.2 \times 10^{-2} z$ (cm) (where $z$ is expressed in centimeters). A 100 nm redshift for a light pulse with $\lambda_0 = 1$ $\mu$m can thus be expected within a propagation length of $z \approx 5$ cm. This estimate suggests that, similar to the regime of a weakly inertial nonlinear response, the waveguide geometry is much more favorable (see, e.g., Refs. [44–47]) for the isolation of the redshift due to the inertial part of optical nonlinearity compared to the tight-focusing geometry. In the regime of filamentation, on the other hand, redshifting due to the initial phase of plasma defocusing, as well as ionization- and shock-wave-induced spectral transformations typically play a much more significant role [20–22], masking effects related to the inertial part of optical nonlinearity. The influence of ionization and shock-wave effects is especially dramatic in the case of few-cycle pulses, when the light field undergoes noticeable spectral transformations within propagation lengths and on a time scale much shorter than the propagation lengths and intervals of time required for the red shift due to the inertial optical nonlinearity. These arguments are consistent with the results of numerical modeling of short-pulse evolution in the filamentation regime in both gas-phase and condensed media [20,21,48]. However, effects related to the inertial optical nonlinearity in the filamentation region can be visualized, as shown by recent experiments [49,50], by probing the filamentation region with a probe pulse delayed in time with respect to the high-intensity field producing a filament.

## V. NONLINEAR PHASE SHIFT IN MATERIALS WITH INHOMOGENEOUSLY DISTRIBUTED MULTIPLE RAMAN-ACTIVE VIBRATIONAL MODES

A single-oscillator model of the inertial nonlinear-optical response [Eq. (12)] yields a Lorentzian Raman gain profile in the spectral domain:

$$g_0(\omega) \propto \omega\gamma[(\omega^2 - \Omega^2)^2 + 4\omega^2\gamma^2]^{-1}, \tag{21}$$

where $\gamma = \tau_2^{-1}$ and $\Omega = (\tau_1^{-2} + \tau_2^{-2})^{1/2}$. Such a Raman gain profile calculated for the time constants of a single-oscillator model of the Raman response of fused silica ($\tau_1 \approx 12.5$ fs, $\tau_2 \approx 32$ fs) is shown by the dashed line in the inset to Fig. 3(a).

For a material where the Raman response cannot be assigned entirely to a single damped oscillator, as suggested by Eq. (12), but is related to a manifold of vibrational modes [51] with a Gaussian distribution of oscillation frequencies, the Raman response function can be represented as [52]

$$h_R(\theta) = \sum_{j=1}^{N} A_j \Theta(\theta) \exp(-\gamma_j \theta) \exp\left(-\frac{\Gamma_j^2 \theta^2}{4}\right) \sin(\omega_j \theta), \tag{22}$$

where $N$ is the number of Raman-active modes, and $A_j$, $\omega_j$, $\gamma_j$, and $\Gamma_j$ are the amplitude, frequency, decay rate, and

Gaussian distribution linewidth of the $j$th Raman-active mode.

In the important particular case of fused silica, which is most frequently used in fiber-optic technologies, the experimental Raman gain can be accurately fitted, as shown by Hollenbeck and Cantrell [52], with Eq. (22) including $N=13$ terms with parameters $A_j$, $\omega_j$, $\gamma_j$, and $\Gamma_j$ specified in Ref. [52]. The Raman gain spectrum calculated by taking the Fourier transform of Eq. (22) with this set of parameters [the solid line in the inset to Fig. 3(a)] provides a very good fit for the experimental Raman gain spectrum, offering a physically transparent explanation for several prominent peaks observed in the experimental Raman spectrum of fused silica that cannot be accounted for with the single-oscillator model of the Raman response [cf. the solid and dashed lines in the inset to Fig. 3(a)]. The series defined by Eq. (22) with parameters as specified in Ref. [52] will be referred to here as the Hollenbeck-Cantrell (HC) model of the Raman response function.

In the HC model of the Raman response, the central peak of the Raman gain observed at approximately 440 $cm^{-1}$ is noticeably narrower and is in a much better agreement with the experimental result than the bandwidth of the Lorentzian Raman gain profile predicted by the single-oscillator model of Eq. (12). Correspondingly, the HC-model Raman response function displays clearly pronounced oscillations within a much longer time interval as compared with the single-oscillator Raman response function, whose oscillations fade off within $\tau_2=32$ fs. In the regime of short light pulses [$\tau_p=20$ fs in Fig. 3(a)], these oscillations with slightly different decay times are readily seen in the temporal profile of the nonlinear phase shift $\varphi_R$ in the trailing edge of the laser pulse. For longer pulses [$\tau_p=100$ fs in Fig. 3(b)], oscillations in $\varphi_R$ on the back of the light pulse are not visible any longer, as they are washed out through the integration over a larger time interval, defined by a longer light pulse [see Eq. (5)]. Still, even in this regime, a slightly stronger inertia of the HC model translates into a slightly larger lag of the temporal profile of the nonlinear phase with respect to the driving light pulse [cf. the dashed line and circles in Fig. 3(b)].

## VI. CONCLUSION

We have shown in this paper that inertia of optical nonlinearity distorts the temporal profile of the intensity-dependent phase shift of an ultrashort laser pulse relative to the phase induced by the instantaneous optical nonlinearity. We demonstrate that a weakly inertial optical nonlinearity, whose response time is smaller than the pulse width, tends to redshift the light field and generates a cubic-phase correction to the quadratic phase, thus complicating the chirp of the spectrally broadened field. These results agree well with the signatures of the Raman effect observed in the phase of ultrashort light pulses using frequency-resolved optical gating [53]. For very short light pulses with pulse widths shorter than the response times of optical nonlinearity, the redshift and cubic-phase terms often dominate the nonlinear phase shift, giving rise to phase profiles significantly different from those induced by instantaneous optical nonlinearity.

## ACKNOWLEDGMENTS

Illuminating discussions with Ferenc Krausz and Eleftherios Goulielmakis are gratefully acknowledged. This study was supported in part by Grant No. RUP2-2695 of the U.S. Civilian Research & Development Foundation for the Independent States of the Former Soviet Union and the Federal Research Program of the Ministry of Science and Education of the Russian Federation.

[1] E. Goulielmakis, V. S. Yakovlev, A. L. Cavalieri, M. Uiberacker, V. Pervak, A. Apolonski, R. Kienberger, U. Kleineberg, and F. Krausz, Science **317**, 769 (2007).
[2] A. M. Zheltikov, Phys. Usp. **49**, 605 (2006).
[3] J. M. Dudley, G. Genty, and S. Coen, Rev. Mod. Phys. **78**, 1135 (2006).
[4] E. Goulielmakis, M. Schultze, M. Hofstetter, V. S. Yakovlev, J. Gagnon, M. Uiberacker, A. L. Aquila, E. M. Gullikson, D. T. Attwood, R. Kienberger, F. Krausz, and U. Kleineberg, Science **320**, 1614 (2008).
[5] *Few-Cycle Laser Pulse Generation and Its Applications*, edited by F. X. Kätner (Springer, Berlin, 2004).
[6] A. M. Zheltikov, A. L'Huillier, and F. Krausz, in *Handbook of Lasers and Optics*, edited by F. Träger (Springer, New York, 2007), pp. 157–248.
[7] Th. Udem, R. Holzwarth, and T. W. Hänsch, Nature (London) **416**, 233 (2002).
[8] J.-X. Cheng and X. S. Xie, J. Phys. Chem. B **108**, 827 (2004).
[9] A. Volkmer, J.-X. Cheng, and X. S. Xie, Phys. Rev. Lett. **87**, 023901 (2001).
[10] A. V. Gorbach and D. V. Skryabin, Phys. Rev. A **76**, 053803 (2007).
[11] D. V. Skryabin, F. Luan, J. C. Knight, and P. S. J. Russell, Science **301**, 1705 (2003).
[12] P. K. A. Wai, H. H. Chen, and Y. C. Lee, Phys. Rev. A **41**, 426 (1990).
[13] V. N. Serkin and A. Hasegawa, Phys. Rev. Lett. **85**, 4502 (2000).
[14] J. C. Travers, A. B. Rulkov, B. A. Cumberland, S. V. Popov, and J. R. Taylor, Opt. Express **16**, 14435 (2008).
[15] V. N. Serkin and A. Hasegawa, IEEE J. Sel. Top. Quantum Electron. **8**, 418 (2002).
[16] V. N. Serkin, A. Hasegawa, and T. L. Belyaeva, Phys. Rev. Lett. **98**, 074102 (2007).
[17] A. M. Zheltikov, Phys. Rev. E **75**, 037603 (2007).
[18] Y. R. Shen, *The Principles of Nonlinear Optics* (Wiley, New York, 1984).
[19] T. Brabec and F. Krausz, Rev. Mod. Phys. **72**, 545 (2000).
[20] L. Bergé, S. Skupin, R. Nuter, J. Kasparian and J.-P. Wolf, Rep. Prog. Phys. **70**, 1633 (2007).
[21] A. Couairon and A. Mysyrowicz, Phys. Rep. **441**, 47 (2007).
[22] E. E. Serebryannikov, E. Goulielmakis, and A. M. Zheltikov,

New J. Phys. **10**, 093001 (2008).
[23] C. P. Hauri, W. Kornelis, F. W. Helbing, A. Heinrich, A. Couairon, A. Mysyrowicz, J. Biegert, and U. Keller, Appl. Phys. B: Lasers Opt. **79**, 673 (2004).
[24] C. Hauri, A. Guandalini, P. Eckle, W. Kornelis, J. Biegert, and U. Keller, Opt. Express **13**, 7541 (2005).
[25] W. M. Wood, C. W. Siders, and M. C. Downer, IEEE Trans. Plasma Sci. **21**, 20 (1993).
[26] B. Rau, C. W. Siders, S. P. Le Blanc, D. L. Fisher, M. C. Downer, and T. Tajima, J. Opt. Soc. Am. B **14**, 643 (1997).
[27] J.-F. Ripoche, H. R. Lange, M. A. Franco, B. S. Prade, P. Rousseau, and A. Mysyrowicz, IEEE J. Sel. Top. Quantum Electron. **4**, 301 (1998).
[28] A. L. Gaeta, Phys. Rev. Lett. **84**, 3582 (2000).
[29] H. Ward and L. Bergé, Phys. Rev. Lett. **90**, 053901 (2003).
[30] T. K. Gustafson, J. P. Taran, H. A. Haus, J. R. Lifsitz, and P. L. Kelley, Phys. Rev. **177**, 306 (1969).
[31] K. J. Blow and D. Wood, IEEE J. Quantum Electron. **25**, 2665 (1989).
[32] F. M. Mitschke and L. F. Mollenauer, Opt. Lett. **11**, 659 (1986).
[33] E. M. Dianov, A. Y. Karasik, P. V. Mamyshev, A. M. Prokhorov, V. N. Serkin, M. F. Stel'makh, and A. A. Fomichev, JETP Lett. **41**, 294 (1985).
[34] G. P. Agrawal, *Nonlinear Fiber Optics* (Academic Press, San Diego, 2001).
[35] J. Santhanama and G. P. Agrawal, Opt. Commun. **222**, 413 (2003).
[36] R. H. Stolen, J. P. Gordon, W. J. Tomlinson, and H. A. Haus, J. Opt. Soc. Am. B **6**, 1159 (1989).
[37] M. Mlejnek, E. M. Wright, and J. V. Moloney, Opt. Lett. **23**, 382 (1998).
[38] A. M. Zheltikov, Opt. Lett. **32**, 2052 (2007).
[39] X. Liu, C. Xu, W. H. Knox, J. K. Chandalia, B. J. Eggleton, S. G. Kosinski, and R. S. Windeler, Opt. Lett. **26**, 358 (2001).
[40] D. T. Reid, I. G. Cormack, W. J. Wadsworth, J. C. Knight, and P. S. J. Russell, J. Mod. Opt. **49**, 757 (2002).
[41] E. E. Serebryannikov, A. M. Zheltikov, N. Ishii, C. Y. Teisset, S. Kohler, T. Fuji, T. Metzger, F. Krausz, and A. Baltuska, Phys. Rev. E **72**, 056603 (2005)
[42] M.-C. Chan, S.-H. Chia, T. —M. Liu, T.-H. Tsai, C. Ho, A. A. Ivanov, A. M. Zheltikov, J.-Y. Liu, H.-L. Liu, and C.-K. Sun, IEEE Photon. Technol. Lett. **20**, 900 (2008).
[43] A. C. Cheung, D. M. Rank, R. Y. Chiao, and C. H. Townes, Phys. Rev. Lett. **20**, 786 (1968).
[44] D. G. Ouzounov, F. R. Ahmad, D. Müller, N. Venkataraman, M. T. Gallagher, M. G. Thomas, J. Silcox, K. W. Koch, and A. L. Gaeta, Science **301**, 1702 (2003).
[45] F. Luan, J. C. Knight, P. St. J. Russell, S. Campbell, D. Xiao and D. T. Reid, B. J. Mangan, D. P. Williams, and P. J. Roberts, Opt. Express **12**, 835 (2004).
[46] D. G. Ouzounov, C. J. Hensley, A. L. Gaeta, N. Venkateraman, M. T. Gallagher, and K. W. Koch, Opt. Express **13**, 6153 (2005).
[47] A. A. Ivanov, A. A. Podshivalov, and A. M. Zheltikov, Opt. Lett. **31**, 3318 (2006).
[48] S. Skupin and L. Bergé, Physica D **220**, 14 (2006).
[49] I. V. Fedotov, A. D. Savvin, A. B. Fedotov, and A. M. Zheltikov, Opt. Lett. **32**, 1275 (2007).
[50] F. Calegari, C. Vozzi, S. Gasilov, E. Benedetti, G. Sansone, M. Nisoli, S. De Silvestri, and S. Stagira, Phys. Rev. Lett. **100**, 123006 (2008).
[51] G. E. Walrafen and P. N. Krishnan, Appl. Opt. **21**, 359 (1982).
[52] D. Hollenbeck and C. D. Cantrell, J. Opt. Soc. Am. B **19**, 2886 (2002).
[53] K. W. DeLong, C. L. Ladera, R. Trebino, B. Kohler, and K. R. Wilson, Opt. Lett. **20**, 486 (1995).